IEEE Access
Multidisciplinary | Rapid Review | Open Access Journal

Received February 4, 2019, accepted March 22, 2019, date of publication April 3, 2019, date of current version April 22, 2019.

Digital Object Identifier 10.1109/ACCESS.2019.2908663

An Innovative Event-Based Filtering Scheme Using H_∞ Performance for Stochastic LTI Systems Considering A Practical Application in Smart Modernized Microgrids

SEYED HOSSEIN MOUSAVI[1], (Member, IEEE), MASOUD DAVARI[2], (Member, IEEE), AND HORACIO J. MARQUEZ[3], (Senior Member, IEEE),

[1]Niigon Machines, Ltd., Vaughan, ON L4H 0S8, Canada
[2]Department of Electrical and Computer Engineering, Allen E. Paulson College of Engineering and Computing, Georgia Southern University, Statesboro Campus, Statesboro, GA 30460, USA
[3]Department of Electrical and Computer Engineering, University of Alberta, Edmonton, AB T6G 2V4, Canada

Corresponding author: Masoud Davari (mdavari@georgiasouthern.edu)

This work was supported by the U.S. National Science Foundation (NSF) provided through the Core Program of Energy, Power, Control, and Networks (EPCN), Division of Electrical, Communications and Cyber Systems (ECCS) under Grant #180827; the idea of S. H. Mousavi's work has been mostly generated when he was with the University of Alberta.

ABSTRACT In this paper, considering both Lyapunov stability and H_∞ performance criteria, a novel event-based filtering scheme is proposed for a class of "stochastic" linear systems with noise, which significantly compromises the performance of event-triggered systems. This paper contributes to the field of research as follows. First, the scheme proposed will reduce data transmission between subsystems while maintaining stability and performance—which is a challenging task in the control of the aforementioned event-triggered systems. Second, it will be shown that our method is robust against stochastic measurement noise—in addition to disturbances—and simultaneously ensures the H_∞ performance of the filter error. Third, the parameters of the triggering scheme will be designed based on the fact that the H_∞ performance of the estimation error is guaranteed in the presence of the exogenous disturbance. At last, but by no means least, the practical aspects of the proposed event-based filtering scheme are considered, especially the practical considerations for the case of modernized grids (also known as smart grids). In this regard, in order to evaluate the proposed methodology's effectiveness, its performance has been examined for two different practical applications with making use of both simulations and experiments; the simulation results of a quarter-car plant model with the suggested method is provided. Afterward, hardware-in-the-loop (HIL) tests will be conducted on a modernized microgrid using the proposed event-based scheme as an application to smart modernized grids of the future.

INDEX TERMS Event-based filter design, event-based observer, exogenous disturbance, H_∞ performance, Lyapunov stability, measurement noise, microgrids, primary frequency control, quarter-car, smart modernized grids, stochastic linear time-invariant (LTI) systems, stochastic noise.

NOMENCLATURE

A. Variable

μ	Expected value of a random variable
ν	Stochastic measurement noise
σ	Standard deviation of a random variable
σ^2	Variance of a random variable
e_F	Estimation error
e_z	Filter error
h	Event-based scheme's clock period for verifying triggering condition
S_P	Simulation period

The associate editor coordinating the review of this manuscript and approving it for publication was Heng Zhang.

SS_R	Sensor sampling rate
T_{int}	Averaging process' time window

B. Set

$\mathbb{R}^+$	Set of positive real numbers
$\mathbb{R}$	Field of real numbers
$\mathbb{N}$	Set of natural numbers
$\mathbb{R}^n$	n dimensional Euclidean space

I. INTRODUCTION

Event-based algorithms employing different signal-processing methodologies, e.g., wavelet, time series, etc., have been used in many areas of engineering—e.g., civil engineering, electrical and computer engineering ranging from communications, controls, and electric power disciplines, etc.—as well as science—e.g., computer science, medicine, etc. [1]–[19].

In control theory, over the last decade, event-triggered systems have emerged as an alternative to the traditional time-triggered sampling schemes. Contrary to the time-triggered case, in an event-based structure, data is communicated across subsystems in an aperiodic fashion by means of some form of triggering mechanism. The primary advantage of event-triggered systems is the potential ability to maintain stability and performance while reducing the transmission of information between subsystems. Concerning the aforementioned problem in control theories—*considering the existence of stochastic noise (which results in stochastic linear time-invariant (LTI) systems)*—none of the signal-processing-based methods are able to guarantee both stability and performance of the event-triggered systems from the standpoint of Lyapunov stability and H_∞ performance. Thus, from all problems in the areas of event-triggered algorithms, this paper focuses on the Lyapunov stability and H_∞ performance of event-based filtering systems for control. To this end, a literature review has been conducted considering the historical background of this problem.

Some recent works (e.g., see [11]–[19] and references therein) have recently dealt with and investigated event-based approaches in control systems. However, none of them have studied event-triggered controls for stochastic LTI systems considering both stability and performance along with the practical aspects associated with the implementation of event-triggered controls on physical power systems—e.g., on smart, modernized grids—which are required to be taken into account in the research. In lights of the aforementioned research needs, this paper has studied and researched into this new problem while taking into account its practical implementations. In this paper, the above-mentioned challenges have been addressed, so it mainly contributes to the research under investigation—i.e., event-based filtering systems in control systems—as follows.

- First, the H_∞ event-based filters for *stochastic* LTI systems, whose output measurements are contaminated by noise are investigated, and an innovative approach for modeling and considering the aforementioned stochastic noise in the event-based control systems is proposed.
- Second, inspired by our previous work in [20], an event-based filtering scheme is proposed which is robust against noise and—at the same time—reduces data transmission from plant to the filter side effectively. To do so, a delay system approach is proposed and used in order to model the error dynamics in this paper.
- Third, triggering scheme parameters are synthesized such that H_∞ performance of the estimation error is guaranteed in the presence of an exogenous disturbance.
- Last, but by no means least, the practical aspect of the proposed event-based filtering scheme is considered and evaluated in order to be applied in smart grids—which is among the key contributions of this research paper.

For the above-mentioned research thrusts, this paper has provided a comprehensive literature review—up to the authors' best knowledge—as follows. Early work on the topic was reported by Åström and Bernhardsson [21]. In this reference, the authors consider a first-order stochastic system and show that using the same average sampling rate, the event-based controller gives a remarkably smaller output variance compared to a periodic controller. Motivated by this result, much research has been done extending the same principles to more general control problems. See for example [22]–[24] and the references therein. More recently, event-based estimation has been the subject of much attention. Several articles consider the problem of event-based filters in the framework of minimum mean squared error (MMSE) or maximum likelihood (ML) estimation (see [25]–[27] to just name a few). In this paper, however, our primary interest is in filter design for continuous-time systems by Lyapunov-based methods. More explicitly, we study H_∞ event-based filter design in the presence of exogenous plant disturbance and measurement noise. In [28]–[30], the authors study this problem for a general class of LTI systems and use a delay system approach to model the system and proceed to design. In [31], a neural-network with nonlinear dynamics is considered and an event-based filter is designed to guarantee a dissipativity property for the estimation error.

In the Lyapunov-based works cited above, both exogenous disturbance and measurement noise are assumed to be square integrable. When looking at the problem of state estimation, however, it is important to distinguish between two classes of perturbations; namely, sensor noise and plant disturbances. Both these signals affect the state estimation process but have very different origins. Disturbance action refers to an exogenous signal affecting the plant (such as the effect of a load in an electric motor or gravitation forces in a robotic manipulator, etc.) and is typically well captured as square-integrable sense. The H_∞ theory, in fact, exploits this assumption and has lead to a comprehensive body of literature and numerous successful applications. Sensor noise, however, constitutes a different type of perturbation which should be treated separately from the disturbance action. More importantly, sensor noise can be particularly harmful in event-triggered systems.

Normally, in an event-triggered system, a new control action is generated whenever changes in the measured signal are above a pre-established threshold. The presence of noise compromises this mechanism by generating false changes (thus, producing unnecessary control actions), or more detrimentally, by producing false negative readings (and thus not generating a signal when one is needed).

With respect to practical applications, the proposed scheme is implemented and tested using one of the most important, integral parts of the electric power sector, which is a microgrid [32]–[35]. Indeed, the electrical power industry has been progressing towards simultaneously integrating more distributed energy resources, renewables, power networks, and energy storage systems (e.g., battery systems) under the umbrella of smart grids [33], [36]–[38]. In this context, the modernized microgrid (MMG) concept brings many benefits to the control, operation, and demands supply within the electric power industry. One of the key elements in smart, modernized grids is having more advanced, sophisticated, modern controls, along with communications, as per the Energy Independence and Security Act of 2007 (EISA-2007), which was approved by the U.S. Congress in January 2007 and signed to law in December 2007 [39]. Event-driven mechanisms can play an integral role in the expansion, implementation, and modernization of currently operating microgrids and power systems as they can reduce the transmission of information between subsystems. Thus, we can add more entities and devices to the control network and to the supervisory control and data acquisition (SCADA) of smart grids with less networked control systems' latency and less concern associated with communication delays. Consequently, an MMG within a smart grid paradigm is a very good candidate for examining the event-driven filter proposed here. In this paper, a two-machine microgrid is employed and tested in order to validate the effectiveness of the proposed event-driven filter.

The remaining of the paper is organized as follows. In section II problem statement is given and our proposed scheme is presented. In Section III the system dynamics is modeled in time delay form and performance analysis is carried out in section IV. Section V contains the design procedure for the scheme parameters. Simulation results are given in section VI, and finally experimental validation for a microgrid is provided in section VII in order to evaluate the efficiency of the system.

A. PRELIMINARIES

$\mathbb{R}^n$ has Euclidean norm denoted by $|x|$. $\mathcal{L}_2[0,T]$ represents the space of square integrable functions over $[0,T]$, i.e., $\mathcal{L}_2[0,T] := \{w(t) : \mathbb{R}^+ \to \mathbb{R}^n | \|w\|_T < \infty\}$, where $\|w\|_T = (\int_0^T |w(t)|^2 dt)^{\frac{1}{2}}$ is the norm of $w \in \mathcal{L}_2$. When the interval $[0,T] = [0,+\infty)$, the norm is denoted $\|w\|$. Given a matrix $A = [a_{ij}]_{n\times n}$, A^T and A^{-1} denote the transpose and inverse of A, respectively. The identity matrix of appropriate dimension is represented by I. In a symmetric matrix, symbol "$\star$" is used to induce symmetric terms.

When random variable ν is Gaussian, the normal distribution of ν is denoted by $\mathcal{N}(\mu, \sigma^2)$ with the expected value of μ and the variance of σ^2.

It is easily proved that for any $x, y \in \mathbb{R}^n$ and any positive definite matrix $D \in \mathbb{R}^{n\times n}$ we have

$$2x^T y \le x^T D x + y^T D^{-1} y. \tag{1}$$

II. PROBLEM STATEMENT

Consider the following continuous-time linear system; for the purpose of problem formulations required to be used in this paper, (2) includes the general form of all linear systems, whose outputs were corrupted by the stochastic measurement noise,

$$\begin{aligned} \dot{x}(t) &= A_p x(t) + B_p w(t), \\ y(t) &= C_p x(t) + \nu(t), \quad z(t) = H_p x(t), \end{aligned} \tag{2}$$

where $x(t) \in \mathbb{R}^n$ is the state vector and $w(t) \in \mathbb{R}^m$ is the exogenous disturbance, which is assumed to belong to $\mathcal{L}_2[0,+\infty)$. $y(t) \in \mathbb{R}^p$ is the measured output contaminated by some stochastic measurement noise $\nu(t)$, and $z(t)$ is the signal to be estimated.

Assumption 1: The measurement noise $\nu(t)$ is a zero mean white Gaussian noise vector with the covariance vector $\sigma^2 I$.

It is assumed the gain L in the following observer has been already designed such that $A_p - LC_p$ is Hurwitz and so the dynamics of estimation error $e_F = x - x_F$ is stable.

$$\begin{aligned} \dot{x}_F(t) &= A_p x_F(t) + L(y_F(t) - y(t)), \\ y_F(t) &= C_p x_F(t), \quad z_F(t) = H_p x_F(t). \end{aligned} \tag{3}$$

The goal of this paper is to modify the above-mentioned observer using an event-based mechanism, such that the transmission of output samples from the plant to the observer side is effectively reduced, while the signal $z_F(t)$ estimates $z(t)$ and the following H_∞ performance holds

$$E\{\|e_F\|_T\} \le \gamma \|w\|_T + \sigma, \quad \forall\, T > 0, \tag{4}$$

where $\sigma \in \mathbb{R}$, and $e_z := z - z_F$ is the filter error.

As mentioned earlier, [29] and [30] consider a Lyapunov approach to design the event-based filters. The triggering condition (TC) in the referred works can be formulated as follows (see [29], [30])

$$(y(t) - \hat{y}(t))^T (y(t) - \hat{y}(t)) \le \beta y^T(t) y(t), \tag{5}$$

where $\hat{y}(t)$ is piecewise constant and denotes the last output sample sent to the observer. Using the above TC, observer (3) has the following event-based form:

$$\begin{aligned} \dot{x}_F(t) &= A_p x_F(t) + L(y_F(t) - \hat{y}(t)), \\ y_F(t) &= C_p x_F(t), \quad z_F(t) = H_p x_F(t). \end{aligned} \tag{6}$$

As inferred from (5), due to the presence of stochastic measurement noise $\nu(t)$ in $y(t)$ and also $\hat{y}(t)$, the traditional TC may trigger unnecessary samples. Therefore, although this triggering condition is simple to implement, it may not be efficient in practical cases, where stochastic noise is present on the measured outputs.

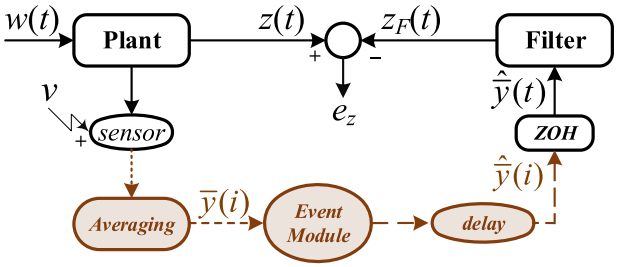

FIGURE 1. Block diagram of the proposed event-based filter.

In the next section, we propose an event-based observer, which is robust against measurement noise and efficiently lowers data communication between plant and observer.

A. PROPOSED EVENT-BASED FILTER SCHEME

We assume that the triggering condition is clock driven with a period of h, and verified at instants ih ($i \in \mathbb{N}$). Denote the triggering instants by $\{k_j\}_{j=1}^{\infty}$. Inspired by our previous work the triggering condition is defined as follows (see [20]):

$$k_{l+1} := \min\{i > k_l : (\bar{y}(i) - \bar{y}(k_l))^T(\bar{y}(i) - \bar{y}(k_l)) - \beta \bar{y}^T(i)\bar{y}(i) \geq 0\}, \quad (7)$$

where $\bar{y}(i)$ represents the average of the output signal $y(t)$ over the time interval $[ih - T_{int}, ih]$ with $T_{int} \in (0, h]$, i.e., $\bar{y}(ih) = \frac{1}{T_{int}} \int_{ih-T_{int}}^{ih} y(\alpha)d\alpha$. Also, $\beta \in \mathbb{R}^+$ is a parameter to be designed using the approach introduced in section V. The block diagram of the proposed filter is shown in Fig. 1 and works as follows: once the TC is violated, an updated value of $\bar{y}(i)$ is transmitted to the filter side. So, both TC and the communicated data use the average values $\bar{y}(i)$. Using equation (2) we have

$$\bar{y}(i) = C_p\bar{x}(i) + \bar{v}(i), \quad (8)$$

where $\bar{v}(i)$ is the average of the noise signal over the time interval $[ih - T_{int}, ih]$. This average value can be approximated as

$$\bar{v}(i) \approx S_{n_s} = \frac{1}{n_s}\sum_{j=1}^{n_s} v_{ij}. \quad (9)$$

In the above equation, the noise samples $\{v_{ij}\}_{j=1}^{n_s}$ are independent random variables with distribution $\mathcal{N}(0, \sigma^2)$ (see Assumption 1), which are collected over the interval $[ih - T_{int}, T_{int}]$. Thus, according to the *Central Limit Theorem*, for large enough number n_s, with a good approximation, the distribution of S_{n_s} can be described as $\mathcal{N}(0, \sigma^2/n_s)$—i.e., with a high probability—$\bar{v}(i)$ takes values in a very small region of origin (see [40] and theorems, as well as references, therein). This means that using average values of measured outputs rather than their instant values one is able to effectively reduce the impact of noise on the triggering condition and also transmitted signal.

III. MODELING THE PROPOSED EVENT BASED SYSTEM

With the event-based structure of the previous section, the dynamics of the filter can be expressed as follows

$$\begin{aligned} \dot{x}_F(t) &= A_p x_F(t) + L(y_F(t) - \hat{\bar{y}}(t)), \\ y_F(t) &= C_p x_F(t), \quad z_F(t) = H_p x_F(t), \end{aligned} \quad (10)$$

where $\hat{\bar{y}}(t)$ is the output of the triggering module and the input to the filter, defined as

$$\hat{\bar{y}}(t) := \bar{y}(k_j) \quad \text{for } t \in [k_j h, k_{j+1}h),\ j \in \mathbb{N}. \quad (11)$$

Using equations (2) and (10), the error dynamics is obtained as

$$\begin{aligned} \dot{e}_F(t) &= (A_p - LC_p)e_F(t) + B_p w(t) + LC_p x(t) - L\hat{\bar{y}}(t), \\ e_z(t) &= H_p e_F(t), \end{aligned} \quad (12)$$

where, the e_z is the filter error.

To analyze the dynamics of system (12), we use a delay system approach. In this regard, the time interval $[0, +\infty)$ is broken down as $[0, +\infty) = \bigcup_{k=1}^{+\infty}[k_j h, k_{j+1}h)$ (see [41] and references therein). Using equations (11) and (8), the error dynamics (12) for $t \in [k_j h, k_{j+1}h)$ can be expressed as

$$\begin{aligned} \dot{e}_F(t) &= (A_p - LC_p)e_F(t) + B_p w(t) + LC_p x(t) \\ &\quad - LC_p\bar{x}(k_j) - L\bar{v}(k_j), \\ e_z(t) &= H_p e_F(t). \end{aligned} \quad (13)$$

Consider the time instant $t \in [k_j h, k_{j+1}h)$ and denote κ_t as the latest sample value before "t," i.e., $\kappa_t = \max\{i \in \mathbb{N} : ih \leq t\}$. Define

$$\tau(t) := t - \kappa_t h, \quad \text{with } 0 \leq \tau(t) \leq h, \quad (14)$$

$$e_t := C_p\bar{x}(\kappa_t) - C_p\bar{x}(k_j). \quad (15)$$

Adding and subtracting $LC_p\bar{x}(\kappa_t)$ on the right-hand side of dynamics equation in (13), and using the above definitions, the error dynamics is modeled in the following time-delay form

$$\begin{aligned} \dot{e}_F(t) &= (A_p - LC_p)e_F(t) + B_p w(t) \\ &\quad + LC_p x(t) + Le_t - LC_p\bar{x}(t - \tau(t)) - L\bar{v}(k_j), \\ e_Z(t) &= H_p e_F(t). \end{aligned} \quad (16)$$

The proposed TC is also written in time-delay form—which is derived by following the steps similar to those in [20]. According to (7) and (8), the following inequalities hold for all i satisfying $k_j \leq i < k_{j+1}$

$$\begin{aligned} &e_t^T e_t + (\bar{v}(i) - \bar{v}(k_j))^T(\bar{v}(i) - \bar{v}(k_j)) + 2e_t^T(\bar{v}(i) - \bar{v}(k_j)) \\ &\quad \leq \bar{x}^T(i)C_p^T\beta C_p\bar{x}(i) + \bar{v}^T(i)\beta\bar{v}(i) + 2\bar{x}^T(i)C_p^T\beta\bar{v}(i). \end{aligned} \quad (17)$$

According to the definition of κ_t, we have $k_j \leq \kappa_t < k_{j+1}$ for all $t \in [k_j h, k_{j+1}h)$. Thus, using this fact and based on (17) we obtain

$$\begin{aligned} &e_t^T e_t + (\bar{v}(\kappa_t) - \bar{v}(k_j))^T(\bar{v}(\kappa_t) - \bar{v}(k_j)) + 2e_t^T(\bar{v}(\kappa_t) - \bar{v}(k_j)) \\ &\quad \leq \bar{x}^T(\kappa_t)C_p^T\beta C_p\bar{x}(\kappa_t) + \bar{v}^T(\kappa_t)\beta\bar{v}(\kappa_t) + 2\bar{x}^T(\kappa_t)C_p^T\beta\bar{v}(\kappa_t), \end{aligned}$$

which using definition (14) can be rewritten as

$$\begin{aligned} e_t^T e_t \le\ & \bar{x}(t-\tau(t))^T C_p^T \beta C_p \bar{x}(t-\tau(t)) \\ & + \bar{v}^T(t-\tau(t))\beta\bar{v}(t-\tau(t)) \\ & + 2\bar{x}^T(t-\tau(t))C_p^T\beta\bar{v}(t-\tau(t)) \\ & - 2e_t^T\bar{v}(t-\tau(t)) + 2e_t^T\bar{v}(k_j). \end{aligned}$$

Applying inequality (1) to $2e_t^T\bar{v}(k_j)$ with $D := I - D_1$ and substituting the result in the above inequality, we have:

$$e_t^T D_1 e_t \le \bar{x}(t-\tau(t))^T C_p^T \beta C_p \bar{x}(t-\tau(t)) + \Delta_v(t), \quad (18)$$

where

$$\begin{aligned} &\Delta_v(t) \\ &= \bar{v}^T(t-\tau(t))\beta\bar{v}(t-\tau(t)) + 2\bar{x}^T(t-\tau(t))C_p^T\beta\bar{v}(t-\tau(t)) \\ &\quad - 2e_t^T\bar{v}(t-\tau(t)) + \bar{v}(k_j)^T(I-D_1)^{-1}\bar{v}(k_j), \end{aligned}$$

and $D_1 \in \mathbb{R}^{p\times p}$ is an arbitrary positive definite matrix, satisfying $I - D_1 > 0$. Having formulated the event-based dynamics and the TC in a proper time-delay format, we are ready to provide the H_∞ performance analysis.

IV. STABILITY AND PERFORMANCE ANALYSIS

Before considering performance, we demonstrate how to approximate the integral term $\bar{x}(t-\tau(t))$ by making use of a simpler form—i.e., the *Trapezoidal rule* (see [42] and approaches discussed therein). Applying the numerical approximation

$$\int_{t-\tau(t)-T_{int}}^{t-\tau(t)} x(\alpha)d\alpha \approx \frac{T_{int}}{2}[x(t-\tau(t)-T_{int}) + x(t-\tau(t))],$$

the following approximation error is obtained: $\frac{T_{int}^3}{12}|x^{(2)}(t-\tau(t)-T_{int})|$. Since a typical practical integration period satisfies $h \ll 1$, the above formulation provides a trustful approximation for $\bar{x}(t-\tau(t))$, while making the analysis rather simple. Thus, the following equation will be used in our analysis

$$\bar{x}(t-\tau(t)) \approx 1/2(x(t-\tau(t)) + x(t-\tau(t)-T_{int})). \quad (19)$$

Remark 1: Note that there are several alternatives to the above-mentioned Trapezoidal rule (for example, see other methods elaborated in [42]), which can provide more accurate estimates. However, these alternatives come at the expense of additional terms and therefore compromise the analysis without significant benefit.

Since the error dynamics (16) contains the terms of $x(t)$, the stability analysis should be carried out by augmenting the plant model. Defining $\mathcal{X}(t) = [x^T(t), e_F{}^T(t)]^T$ and using (2), (16), and (19) the overall dynamics of the system can be expressed as follows

$$\begin{aligned} \dot{\mathcal{X}}(t) &= A\mathcal{X}(t) + A_{d1}\mathcal{X}(t-\tau(t)) + A_{d2}\mathcal{X}(t-\tau(t)-T_{int}) \\ &\quad + B_e e_t + B_w w + B_v\bar{v}(k_j), \\ e_z(t) &= H\mathcal{X}(t), \end{aligned} \quad (20)$$

where

$$A = \begin{bmatrix} A_p & 0 \\ LC_p & A_p - LC_p \end{bmatrix}, \quad A_{d1} = \begin{bmatrix} 0 & 0 \\ -1/2LC_p & 0 \end{bmatrix},$$
$$A_{d2} = \begin{bmatrix} 0 & 0 \\ -1/2LC_p & 0 \end{bmatrix}, \quad B_e = \begin{bmatrix} 0 & L \end{bmatrix}^T,$$
$$B_w = \begin{bmatrix} B_p & B_p \end{bmatrix}^T \quad B_v = \begin{bmatrix} 0 & -L \end{bmatrix}^T, \quad H = \begin{bmatrix} 0 & H_p \end{bmatrix}.$$

Theorem 1 given below, provides sufficient conditions in form of LMIs to guarantee H_∞ performance for the proposed event-based system.

Theorem 1: Consider the stochastic event-based filter (10), implemented with the proposed triggering condition (7) for the system (2). If there exist matrices D_1 (satisfying $I - D_1 > 0$), $D_2 > 0$, $P > 0$, $Q_i > 0$, $R_i > 0$, U_i and V_i $(i = 0, 1)$ with appropriate dimensions such that the following LMIs hold, then the H_∞ performance (4) is guaranteed for the filter error.

$$\mathcal{L}_j^U = \begin{bmatrix} \Gamma_0 + \Pi + \Pi^T & \star & \star & \star \\ \Gamma_0^R & -R_0 & \star & \star \\ \Gamma_1^R & 0 & -R_1 & \star \\ \Gamma_j^U & 0 & 0 & -R_j \end{bmatrix} < 0, \quad (21)$$

$$\mathcal{L}_j^V = \begin{bmatrix} \Gamma_0 + \Pi + \Pi^T & \star & \star & \star \\ \Gamma_0^R & -R_0 & \star & \star \\ \Gamma_1^R & 0 & -R_1 & \star \\ \Gamma_j^V & 0 & 0 & -R_j \end{bmatrix} < 0, \quad (22)$$

for $j = 0, 1$, where, Γ_0, Π, Γ_j^U, Γ_j^R, Γ_{01}, Γ_{02}, C, and Λ, as shown at the top of the next page.

Proof: Consider the Lyapunov Krasovskii functional $V = \sum_{i=1}^{3} V_i$, where $V_1 = \mathcal{X}(t)^T P\mathcal{X}(t)$, $V_2 = \sum_{j=0}^{1}\int_{t-h-jT_{int}}^{t}\mathcal{X}^T(s)Q_j\mathcal{X}(s)ds$, and $V_3 = \sum_{j=0}^{1}\int_0^{h+jT_{int}}\int_{t-\theta}^{t}\dot{\mathcal{X}}^T(s)R_j\dot{\mathcal{X}}(s)ds d\theta$. Define $\zeta(t) := [\mathcal{X}^T(t),\ \mathcal{X}_\tau^T,\ \mathcal{X}_M^T,\ w^T,\ e_t^T,\ \bar{v}^T]$, with $\mathcal{X}_\tau^T = [\mathcal{X}^T(t-\tau(t)),\ \mathcal{X}^T(t-\tau(t)-T_{int})]$ and $\mathcal{X}_M^T = [\mathcal{X}^T(t-h),\ \mathcal{X}^T(t-h-T_{int})]$. Computing the derivative of V_i along the trajectories of e and x for $t \in [k_j h, k_{j+1}h)$ we have

$$\dot{V}_1 = \zeta^T\Lambda^T P\mathcal{X} + \mathcal{X}^T P\Lambda\zeta, \quad (23a)$$

$$\dot{V}_2 = \sum_{j=0}^{1}\mathcal{X}(t)^T Q_j\mathcal{X}(t) - \sum_{j=0}^{1}\mathcal{X}^T(t-h-jT_{int})Q_j\mathcal{X}(t-h-jT_{int}), \quad (23b)$$

$$\dot{V}_3 = \sum_{j=0}^{1}(h+jT_{int})(\zeta^T\Lambda^T R_j\Lambda\zeta) - \sum_{j=0}^{1}\int_0^{h+jT_{int}}\dot{\mathcal{X}}(t-\theta)^T R_j\dot{\mathcal{X}}(t-\theta)d\theta. \quad (23c)$$

$$\Gamma_0 = \begin{bmatrix} \Gamma_{01} & PA_{d1} & PA_{d2} & 0 & 0 & PB_w & PB_e & PB_v \\ \star & \Gamma_{02} & \Gamma_{04} & 0 & 0 & 0 & 0 & 0 \\ \star & \star & \Gamma_{03} & 0 & 0 & 0 & 0 & 0 \\ \star & \star & \star & -Q_1 & 0 & 0 & 0 & 0 \\ \star & \star & \star & \star & -Q_2 & 0 & 0 & 0 \\ \star & \star & \star & \star & \star & -\gamma^2 & 0 & 0 \\ \star & \star & \star & \star & \star & \star & -D_1 & 0 \\ \star & \star & \star & \star & \star & \star & \star & -D_2 \end{bmatrix},$$

$$\Pi = \begin{bmatrix} V_0 + V_1 & U_0 - V_0 & U_1 - V_1 & -U_0 & -U_1 & 0 & 0 & 0 \end{bmatrix},$$

$$\Gamma_j^U = \sqrt{2h + T_{int}}U_j, \quad \Gamma_j^V = \sqrt{2h + T_{int}}V_j \text{ for } j = 0, 1,$$

$$\Gamma_j^R = \sqrt{h + jT_{int}}R_j\Lambda \quad \text{for } j = 0, 1,$$

$$\Gamma_{01} = A^T P + PA + Q_1 + Q_2 + H^T H,$$

$$\Gamma_{02} = 1/4\beta C^T C, \quad \Gamma_{03} = 1/4\beta C^T C, \ \Gamma_{04} = 1/4\beta C^T C,$$

$$C = \begin{bmatrix} C_p & 0 \end{bmatrix},$$

$$\Lambda = \begin{bmatrix} A & A_{d1} & A_{d2} & 0 & 0 & B_w & B_e & B_v \end{bmatrix}.$$

Using Leibniz-Newton formula and using the approach given in [43], for any U_j and V_j (for $j = 0, 1$) of proper dimensions, we have

$$\zeta^T U_j(\mathcal{X}(t - \tau(t) - jT_{int}) - \mathcal{X}(t - jT_{int} - h) - \int_{t-jT_{int}-h}^{t-jT_{int}-\tau(t)} \dot{\mathcal{X}}(s)ds) = 0,$$

$$\zeta^T V_j(\mathcal{X}(t) - \mathcal{X}(t - jT_{int} - \tau(t)) - \int_{t-\tau(t)-jT_{int}}^{t} \dot{\mathcal{X}}(s)ds) = 0.$$

Applying the above equations in left-hand side of $\dot{V}_3$ in (23c) and after some computation we get

$$\dot{V}_3 \le \sum_{j=0}^{1}(h + jT_{int})(\zeta^T \Lambda^T R_j \Lambda\zeta) + \zeta^T(\Pi + \Pi^T)\zeta + \sum_{j=0}^{1}[(h - \tau(t))\zeta^T U_j R_j^{-1} U_j^T \zeta + (\tau(t) + jT_{int})\zeta^T V_j R_j^{-1} V_j^T \zeta] \quad (24)$$

Now, based on (23a), (23b), (24), and using the fact that the triggering inequality (18) holds for all $t \in [k_j h, k_{j+1}h)$, we have

$$\dot{V} - \gamma^2 w^T w + e_z^T e_z \le \zeta^T(\Gamma_0 + \Pi + \Pi^T)\zeta + \bar{v}(k_j)^T D_2 \bar{v}(k_j) + \sum_{j=0}^{1}(h + jT_{int})\zeta^T \Lambda^T R_j (R_j)^{-1} R_j \Lambda\zeta + \Delta_v(t) + \sum_{j=0}^{1}[(h - \tau(t))\zeta^T U_j R_j^{-1} U_j^T \zeta + (\tau(t) + jT_{int})\zeta^T V_j R_j^{-1} V_j^T \zeta],$$

where $D_2 > 0$ is an arbitrary matrix. The above inequality can be rewritten as

$$\dot{V} - \gamma^2 w^T w + e_z^T e_z \le \zeta^T \bar{\Gamma}\zeta + \bar{v}(k_j)^T D_2 \bar{v}(k_j) + \Delta_v(t), \quad (25)$$

where

$$\bar{\Gamma} = \Gamma_0 + \Pi + \Pi^T + \sum_{j=0}^{1} \Gamma_j^{R^T} R_j^{-1} \Gamma_j^R + \sum_{j=0}^{1}[\frac{h - \tau(t)}{2h + T_{int}} \Gamma_j^U R_j^{-1} \Gamma_j^{U^T} + \frac{\tau(t) + jT_{int}}{2h + T_{int}} \Gamma_j^V R_j^{-1} \Gamma_j^{V^T}]. \quad (26)$$

Since

$$\sum_{j=0}^{1}[\frac{h - \tau(t)}{2h + T_{int}} + \frac{\tau(t) + jT_{int}}{2h + T_{int}}] = 1, \quad (27)$$

equation (26) can be expressed as follows

$$\bar{\Gamma} = \sum_{j=0}^{1}[\frac{h - \tau(t)}{2h + T_{int}} \bar{\Gamma}_j^U + \frac{\tau(t) + jT_{int}}{2h + T_{int}} \bar{\Gamma}_j^V], \quad (28)$$

where $\bar{\Gamma}_j^U = \Gamma_0 + \Gamma_1 + \Gamma_1^T + \Gamma_j^U R_j^{-1} \Gamma_j^{U^T} + \sum_{j=0}^{1} \Gamma_j^{R^T} R_j^{-1} \Gamma_j^R,$

$$\bar{\Gamma}_j^V = \Gamma_0 + \Gamma_1 + \Gamma_1^T + \Gamma_j^V R_j^{-1} \Gamma_j^{V^T} + \sum_{j=0}^{1} \Gamma_j^{R^T} R_j^{-1} \Gamma_j^R.$$

It follows from equation (25) that

$$E\{\dot{V} - \gamma^2 w^T w + e_z^T e_z\} \le E\{\zeta^T \bar{\Gamma}\zeta\} + E\{\bar{v}(k_j)^T D_2 \bar{v}(k_j)\} + E\{\Delta_v(t)\}. \quad (29)$$

Since the elements of the random vector $\bar{v}$ are statistically independent, we have

$$E\{\bar{v}(k_j)^T D_2 \bar{v}(k_j)\} = tr(D_2)\sigma^2/n_s,$$

and for the last term

$$E\{\Delta_v(t)\} = (\beta + tr((I - D_1)^{-1}))\sigma^2/n_s + E\{2\bar{x}^T(t-\tau(t))C_p^T\beta\bar{v}(t-\tau(t)) - 2e_t^T\bar{v}(t-\tau(t))\}.$$

From the system dynamics, it can easily get that the vectors $\bar{x}(t-\tau(t))$ and e_t are independent from $\bar{v}(t-\tau(t))$ and so the last term in above equation is zero. Therefore

$$E\{\Delta_v(t)\} + E\{\bar{v}(k_j)^T D_2 \bar{v}(k_j)\} = c_v/n_s, \tag{30}$$

with

$$c_v = (\beta + tr((I - D_1)^{-1}) + tr(D_2))\sigma^2. \tag{31}$$

From (27) and (28), it is inferred that $\bar{\Gamma}$ is a convex combination $\bar{\Gamma}_0^U$, $\bar{\Gamma}_1^U$, $\bar{\Gamma}_0^V$ and $\bar{\Gamma}_1^V$. Consequently, by using this fact and Schur complement [44], the LMIs (21) and (22) are equivalent to

$$\bar{\Gamma} < 0. \tag{32}$$

Then, from (29), (30) and (32) it is obtained that

$$E\{\dot{V}\} + E\{e_z^T e_z - \gamma^2 w^T w\} \leq -\theta E\{\|x(t)\|^2\} + c_v/n_s, \tag{33}$$

where $-\theta := \max_{0\leq\tau(t)\leq h}(\sum_{j=0}^{1}[\frac{h-\tau(t)}{2h+T_{int}}\theta_j^U + \frac{\tau(t)+jT_{int}}{2h+T_{int}}\theta_j^V])$, with $\theta_j^U = \lambda_{max}(\bar{\Gamma}_j^U)$ and $\theta_j^V = \lambda_{max}(\bar{\Gamma}_j^V)$.

To prove the H_∞ performance, integrate both sides of (33) from k_jh to $T \in [k_jh, k_{j+1}h)$ to obtain $E\{V(T)\} - E\{V(k_jh)\} + E\{\int_{k_jh}^{T} e_z(t)^T e_z(t)dt\} \leq \gamma^2 \int_{k_jh}^{T} w(t)^T w(t)dt + c_v(T - k_j)/n_s$ Repeating the integration operation over the intervals $[k_i, k_{i+1})$ (for $i = 1, \ldots, j-1$), adding each side of the obtained inequalities together, and since $E\{V(T)\}$ is positive, we get

$$E\{\|e_z\|_T^2\} \leq \gamma^2\|w\|_T^2 + E\{V(0)\} + Tc_v/n_s. \tag{34}$$

This concludes the proof. □

Remark 2: Practically speaking, because of the finiteness of the sample numbers n_s, the term Tc_v/n_s in (34) is not exactly equal to zero. However, this bias term can be made sufficiently small by increasing the number of samples, used for the averaging task.

V. PARAMETERS DESIGN

Our event-based system includes the following design parameters: observer gain L, sampling time h, integration time T_{int}, triggering coefficient β and H_∞ gain γ. The sampling time h represents the minimum possible transmission time between two consecutive data points sent to the observer side and, practically, this parameter should be chosen based on the network medium properties, such as transmission rate. T_{int}, plays a key role in suppressing the noise impact on the triggering condition. Depending on the measurement sensor sampling rate, T_{int} should be such that n_s (number of samples in the integration interval) is large enough to make the averaging task (9) more effective.

Next, design L, β and γ in two separate steps. First, assuming an observer has been designed using any methodology for the continuous-time systems resulting in a stable observer (i.e., the eigenvalues of $A_p - LC_p$ have negative real part). Second, β and γ are designed as follows. Based on the definition of the triggering condition in (7), one can infer that the larger β, the less data is transmitted through the network channel. However, the lower convergence rate of estimation error and less disturbance attenuation (bigger γ) are expected. Thus, there is a trade-off in designing β and γ. To assign proper values for these variables, we iteratively solve the following optimization problem for different values of β (starting from zero to the value whose constraints are infeasible) and find the trade-off curve.

$$\begin{aligned} &\min \gamma^2 \\ &\mathcal{L}_0^U < 0, \quad \mathcal{L}_0^V < 0, \\ &\mathcal{L}_1^U < 0, \quad \mathcal{L}_1^V < 0, \end{aligned} \tag{35}$$

where, $\mathcal{L}_j^U$ and $\mathcal{L}_j^V$ $(j = 0, 1)$ are defined as (21) and (22).

VI. SIMULATION RESULTS FOR A QUARTER-CAR

Referred to (2), consider the following dynamics matrices of a quarter-car model with an active suspension (see [29]—from which the below-mentioned dynamics matrices have been borrowed)

$$\begin{aligned} A_p &= [0, 0, 1, -1; 0, 0, 0, 1; -k_s/m_s, 0, -c_s/m_s, c_s/m_s; \\ &\quad k_s/m_u, k_u/m_u, c_s/m_u, -c_s/m_u], \\ B_p &= [0; -2\pi q_0\sqrt{G_0 v}; 0; 0], \; C_p = [0, 0, 0, 1], \\ H_p &= [0, 0, 0.2, 0], \end{aligned}$$

where $m_s = 973$, $k_s = 42720$, $c_s = 3000$, $k_u = 101115$, $m_u = 114$, $G_0 = 512 \times 10^{(-6)}$, $q_0 = 0.1$, $m_u = 114$. Readers are referred to [29] for a detailed explanation of the parameters obtained.

We begin our design by setting the sampling and integration time to 0.05 and 0.02, respectively. In other words, referred to our previously mentioned parameters, h has been set 0.05, and T_{int} has been selected 0.02 for our simulations in this section; it is noteworthy that h is the period of the clock for verifying TC in our filtering scheme and that T_{int} is the time window over which the averaging process task is computed. To achieve an acceptable convergence rate and based on the approach of section V, the filter gain is set to $L = \begin{bmatrix}-1.1320 & -0.5994 & 24.6167 & 18.4649\end{bmatrix}^T$. Implementing the optimization problem (35) for different values of β, between 0 and 1, where the constraints become infeasible. Fig.2 shows the trade-off betweenγ versus β. As expected, a higher attenuation level (smaller γ) demands more data transmission over the network (smaller β).

In order to verify the effectiveness of our approach and compare the method proposed in this paper with other commonly used approaches (e.g., the traditional TC (5) mentioned in [28]–[30]), our event-based filter has been implemented, and the simulation results have been compared

TABLE 1. Number of data sent from plant to the observer.

	Traditional scheme	Proposed scheme with different SS_Rs Hz			
		200	700	1000	5000
$\beta = 0.4$	97	77	65	62	57
$\beta = 0.7$	81	61	49	42	36

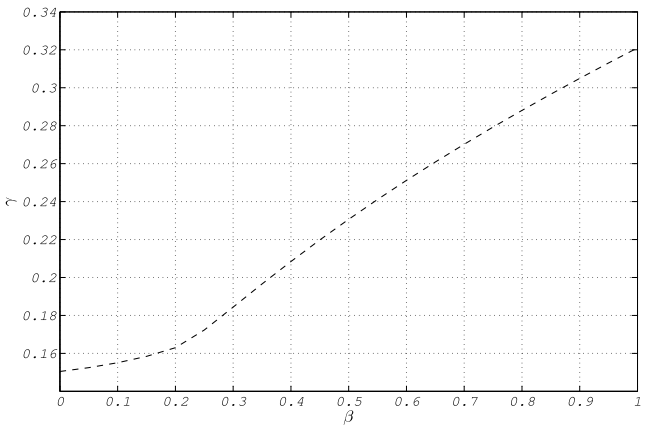

FIGURE 2. Trade-off curve between β and γ.

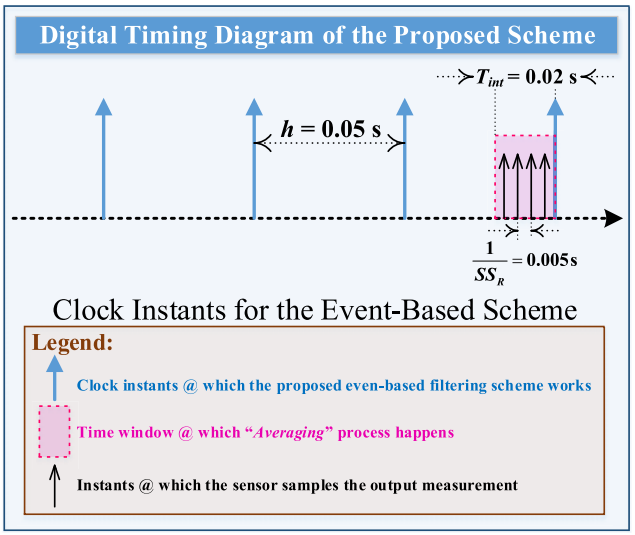

FIGURE 3. The digital timing diagram of the proposed filtering scheme for the case of SS_R = 200 Hz referred to Table 1, just as an instance.

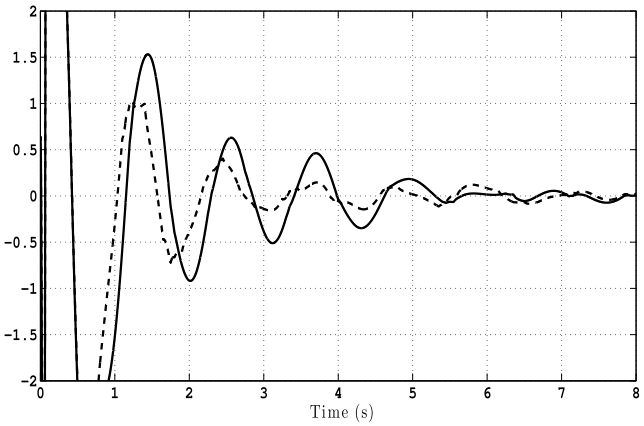

FIGURE 4. Estimation error trajectories for the cases which $\beta = 0.7$ (solid) and $\beta = 0.4$ (dashed)—while using the event-based observer proposed in this paper.

with those of a similar observer while using the traditional TC (5)—given in [29] and [30]). It has been assumed that the output measurement is contaminated by a white Gaussian noise with a distribution of $\mathcal{N}(0, 0.6^2)$, and the disturbance signal is $w(t) = 5e^{-0.1t}sin(4t)$. The initial conditions are set to $x(0) = [-12, 6, 3, 9]^T$ and $x_F(0) = [-3, 3, 0, 0]^T$, and simulations are carried out for 8 s (the simulation period is denoted by S_P hereinafter). Simulations have been carried out using different sensor sampling rates (the sensor sampling rate is denoted by SS_R hereinafter)—in order to clarify the importance of this parameter. In order to furthermore elaborate on the aforementioned parameters for the case of $SS_R = 200$ Hz illustratively—just as an explanatory example—Fig. 3 has demonstrated different parameters via a descriptive "digital timing diagram" for the proposed filtering scheme. As Fig. 3 shows, for our simulations (for which h = 0.05 s and $Tint = 0.02$ s) there are four samples provided by the sensor because $SSR = 200$ Hz—and hence $\frac{T_{int}}{\frac{1}{SS_R}} = 4$ #s. Definitely, for other sensors whose SSRs are higher in Table (1), this number will grow. The number of data transmission points from the plant side to the observer is given in Table 1. When $\beta = 0.7$, the traditional event-based scheme, sends 81 data points to the observer. In other words, the TC is violated at 51% of the number of TC-verifying instants—which is calculated by $0.51 \times \frac{S_P}{h} = 0.51 \times \frac{8.00}{0.05} = 0.51 \times 160 \approx 81$ #s for our simulations. However, utilizing our proposed triggering condition—i.e., *TC (7)*—one is able to reduce this triggering percentage down to 22.5%—i.e., *below half*—depending on the sampling rate chosen for the event generator module. A similar conclusion can be reached for other values of β. Note that from the table, increasing β one can reduce the number of triggering samples. However, this would happen at the expense of lowering the estimation error convergence rate and disturbance attenuation level—something which has obviously been demonstrated in Fig.4.

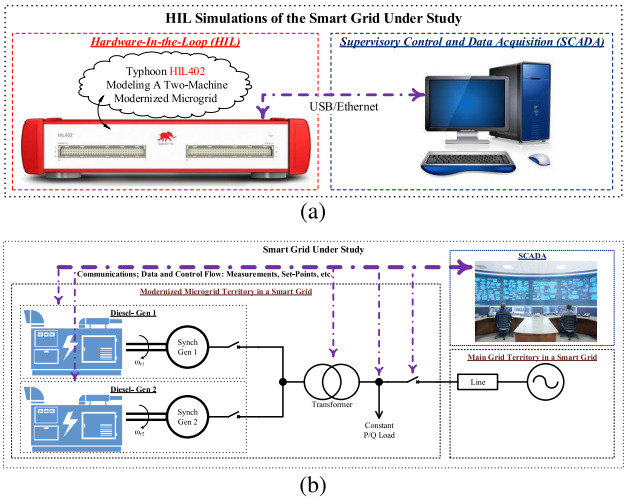

FIGURE 5. Experimental setup: (a) The HIL setup (b) The implemented smart grid using HIL setup for conducting the experiments.

VII. HARDWARE-IN-THE-LOOP TESTING FOR MODERNIZED MICROGRIDS

Hardware-in-the-loop (HIL) systems have found a wide range of applications in smart grids, power systems, power electronic systems, automotive industry, motion control, mechatronics, and robotics because they can provide ultra-high-fidelity simulations. HIL experimental methods are revolutionizing test engineering in many disciplines, including, but not limited to, smart grids, vehicle and communication systems, civil structures, robotics, aerospace systems, and process controls [45], [46]. To examine the effectiveness of the proposed mechanism, we have implemented a two-machine MMG on an HIL402 device from Typhoon HIL Inc. [47] and tested the proposed event-driven filter under the umbrella of smart grids. To this end, we have tested the aforementioned smart grid employing the event-driven filter to investigate its performance under the islanded mode of operation of the formed MMG in frequency control mode. The complete configuration is shown in Fig. 5.

Typhoon HIL402 with 4 processing cores, 16 analog outputs, 16 digital inputs, and 16-bit resolution is tailored for the most demanding microgrid and controller test, verification, and pre-certification tasks. It can test the event-triggered filter with high fidelity, including 20ns sampling HIL, and infinitesimal latency, i.e., 1 μs resulting in emulation errors and latency so small that result in a negligible difference between the real smart grid and HIL emulator measured waveforms. Moreover, using the HIL402 it is possible to simulate our numerical signals with multiple execution rates and improve the overall performance of our digitally simulated HIL system by maximizing the use of available resources. The built-in multi-rate interval overrun monitor closely supervises real-time execution and informs the user in case of potential performance issues. This feature is ideal to test the

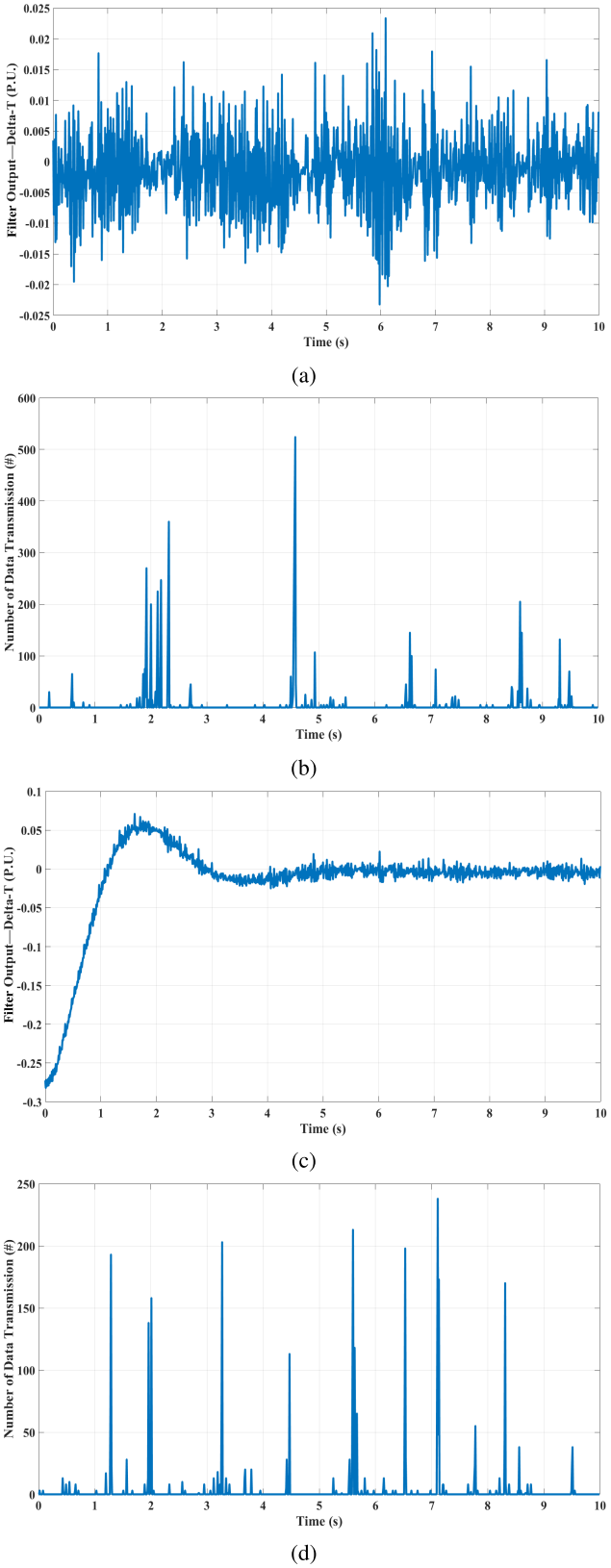

FIGURE 6. Test case one: (a) filter output in per unit (pu) without disturbance; (b) data transmission without disturbance; (c) filter output in pu with disturbance, and (d) data transmission with disturbance.

performance of an event-driven mechanism—similar to the one proposed here in this paper. HIL402 leverages a small simulation time step and advanced numerical algorithms for extremely-wide-dynamic-range models. It emulates fast switching dynamics with a simulation time step, as low as 0.5 μs, and has a full peace of mind that the part of our model with extremely long time constants will run beautifully as well. Indeed, advanced numerical algorithms in HIL402 handle the wide dynamic range models masterfully and run for weeks on end.

The state-space model of a two-machine MMG is given by

$$\begin{aligned}
\dot{\Delta\delta_i} &= \Delta\omega_i, \\
\dot{\Delta\omega_i} &= -\frac{D_i}{2H_i}\Delta\omega_i + \frac{\omega_0}{2H_i}\Delta P_{mi} - \frac{\omega_0}{2H_i}\Delta P_{ei}, \\
\dot{\Delta P_{mi}} &= -\frac{k_i}{T_i}\Delta\omega_i - \frac{1}{T_i}\Delta P_{mi} + \frac{1}{T_i}u_i + \frac{1}{T_i}w_i, \qquad (36)
\end{aligned}$$

where $\Delta\delta_i$, $\Delta\omega_i$, ΔP_{mi}, and ΔP_{ei} are the deviations of rotor angle, relative rotor speed, mechanical input power, and active power of the ith generator, respectively (see [48]–[50] and references therein). The control signal u_i represents the deviation of the valve opening. w_i denotes the disturbance related to control signal. H_i, D_i, ω_0, k_i and T_i are constant system parameters for i=1,2. The active power ΔP_{e1} can be calculated as

$$\Delta P_{e1} = \frac{|E_1||E_2|}{X}[\sin(\delta_1 - \delta_2) - \sin(\delta_{10} - \delta_{20})], \qquad (37)$$

where $\Delta P_{e2} = \Delta P_{e1}$, δ_{10} and δ_{20} are the steady state angles of the first and second generators, and $|E_1|$ and $|E_2|$ are amplitudes of voltage phasors E_1 and E_2. The second synchronous generator is treated as dynamic uncertainty, and has a fixed controller $u_1 = k_{p_1}\Delta\omega_1 + k_{i_1}\dot{\omega_1}$ and $u_2 = k_{p_2}\Delta\omega_2 + k_{i_2}\dot{\omega_2}$, with $k_{p_1}, k_{i_1}, k_{p_2}$, and k_{i_2} as its controller gains. We assume the following parameter values: $D_1 = 1$ Nms, $H_1 = 3$ MJ/MVA, $\omega_0 = 376.99112$ rad/s, $k_1 = 10$, $T_1 = 5.74$ ms, and $D_2 = 1$ Nms, $H_2 = 3$ MJ/MVA, $k_2 = 10$, $T_2 = 5.74$ ms. The simulation time step of the HIL setup is set to 4 μs, and considering the triggering condition criterion in addition to real-time simulation requirements, h and the sensor sampling rate (directly associated with T_{int} of the triggering condition) are set to 80 μs and 6.9769 kHz, for the first test and 80 μs and 28.280 kHz, for test second, as described below. Defining the state $x = \left[\Delta\delta_1, \Delta\omega_1, \Delta P_{m1}, \Delta\delta_2, \Delta\omega_2, \Delta P_{m2}\right]^T$ results in the following matrices associated with the total dynamic system, referred to (2),

$$A_p = \begin{bmatrix}
0 & 1 & 0 & 0 & 0 & 0 \\
0 & \frac{-D_1}{2H_1} & \frac{\omega_0}{2H_1} & 0 & 0 & 0 \\
0 & \frac{-k_1}{T_1} & \frac{-1}{T_1} & 0 & 0 & 0 \\
0 & 0 & 0 & 0 & 1 & 0 \\
0 & 0 & 0 & 0 & \frac{-D_2}{2H_2} & \frac{\omega_0}{2H_2} \\
0 & 0 & 0 & 0 & \frac{-k_1}{T_2} & \frac{-1}{T_2}
\end{bmatrix}, \quad B_p = \begin{bmatrix}
0 \\ 0 \\ \frac{1}{T_1} \\ 0 \\ 0 \\ \frac{1}{T_2}
\end{bmatrix},$$

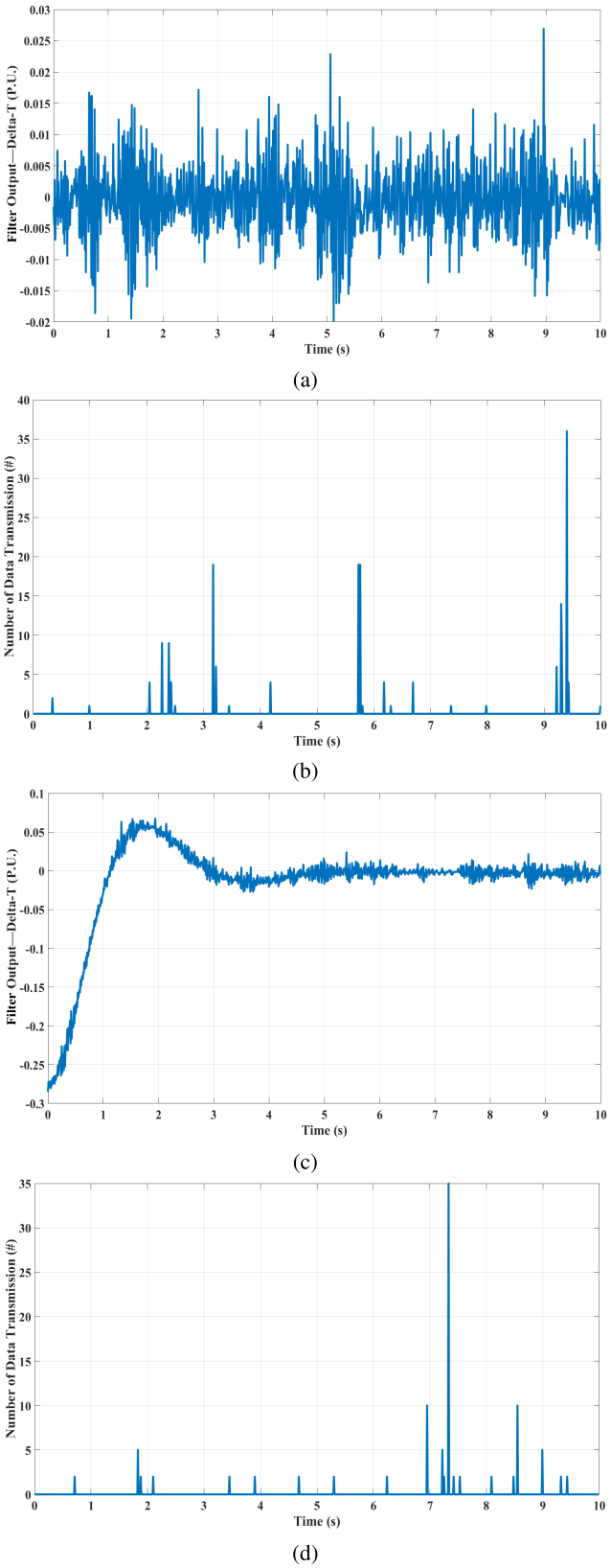

FIGURE 7. Test case two: (a) filter output in pu without disturbance; (b) data transmission without disturbance; (c) filter output in pu with disturbance; and (d) data transmission with disturbance.

$$C_p = \begin{bmatrix} 1 & 1 & 0 & 1 & 1 & 0 \end{bmatrix},$$
$$H_p = \begin{bmatrix} 0 & 0 & 1 & 0 & 0 & 0 \end{bmatrix}. \quad (38)$$

The measured output $y = \Delta\delta_1 + \Delta\omega_1 + \Delta\delta_2 + \Delta\omega_2 + \nu$ is used to estimate the signal $z = \Delta P_{m1}$ using the event-based filter, and accordingly find the torqueΔT_1, given by (39),

$$\Delta T_1 = \frac{1}{\omega_{\text{mech0}}}\Delta P_{m1} - \frac{P_{m1-0}}{\omega^2_{\text{mech0}}}\Delta\omega_{\text{mech1}},$$
$$\omega_{\text{mech0}} = \frac{\omega_0}{p}, \quad \Delta\omega_{\text{mech1}} = \frac{\Delta\omega 1}{p}, \quad (39)$$

where p is the machine number of pole pairs. Experimental results are shown in Figs. 6 and 7. The filter gain was set to $L = [1, 825.6173, -51.3746, 1, 825.6173, -51.3746]^T$. The parameters are $T_{int} = h = 80\ \mu$s and the optimization problem (35) was solved for $\beta = 0.001$. To test the role of the sensor sampling rate and to examine the effectiveness of the filter, two test cases with different SS_R are considered, namely: (i) Test Case One (1): sensor bandwidth is 6.98 kHz, and (ii) Test Case Two (2): sensor bandwidth is 28.28 kHz. In test number one (1), two scenarios were implemented, with and without power disturbance w_i $(i = 1, 2)$. The results are shown in Fig. 6. We see that the *average* of the data-transmission period for these cases are 2.8 ms and 4 ms, respectively. In test case number two (2), again, two scenarios have been implemented, with and without power disturbance w_i $(i = 1, 2)$. The results are shown in Fig. 7, where the average of data transmission period are respectively 56.8 ms and 99 ms. The results validate the efficiency of our proposed scheme in data communication reduction. Moreover, comparing data communication periods for case two with the corresponding numbers of case one illustrates the role of sensor sampling rate increase in the improvement of overall performance.

VIII. CONCLUSION

This paper has proposed an innovative event-triggered filtering scheme using Lyapunov stability and H_∞ performance for noisy, stochastic LTI systems. Considering this fact that it is a challenging task to maintain both the stability and the performance in event-triggered systems, the scheme proposed for linear systems in this research has satisfactorily reduced the number of data transmission between subsystems while preserving the stability and the performance. It was shown that the proposed triggering scheme is robust against measurement noise and also simultaneously guarantees the H_∞ performance for the filter error. The practical aspects of and considerations for implementing the proposed event-based filtering scheme was taken into account. Concerning this, simulation results for a quarter-car model were given to verify the effectiveness of the system; the filter was also experimentally evaluated by making use of it in a modernized microgrid within the paradigm of smart grids implemented on an HIL platform. The applied HIL setup was appropriately designed for event-driven applications as it employed multiple execution rates for real-time simulations. The experimental results demonstrated the effectiveness of the suggested event-triggered scheme.

With the comprehensive analysis and the successful implementation of the event-based algorithm in a purely theoretical setting proposed here, the next logical step would be to consider the same problem for ''nonlinear systems,'' ''hidden Markov models,'' and ''Markov jump linear parameter varying systems.'' As regards these systems, they have much more complicated and challenging mathematical models, for which we need to thoroughly conduct this research on the event-based methodologies—*theoretically, mathematically, and practically*. It is noteworthy that considering and tackling the very well-known ''separation principle'' in nonlinear systems and the channel transmission's unreliability (in addition to the possible nonsynchronous mode variations between the system and the designed filter) bring additional challenges to the problem formulation associated with the aforementioned future research works and investigations.

REFERENCES

[1] S. M. LaConte, S.-C. Ngan, and X. Hu, ''Wavelet transform-based Wiener filtering of event-related fMRI data,'' *Magn. Reson. Med.*, vol. 44, no. 5, pp. 746–757, Nov. 2000.
[2] P. Kovács, V. Carboneb, and Z. Vörös, ''Wavelet-based filtering of intermittent events from geomagnetic time-series,'' *Planet. Space Sci.*, vol. 49, no. 12, pp. 1219–1231, Oct. 2001.
[3] C. Varadharajan, ''A wavelet-based system for event detection in online real-time sensor data,'' M.S. thesis, Dept. Civil Environ. Eng., Massachusetts Inst. Technol., Cambridge, MA, USA, Jan. 2004.
[4] E. Glassman, ''A wavelet-like filter based on neuron action potentials for analysis of human scalp electroencephalographs,'' *IEEE Rev. Biomed. Eng.*, vol. 11, no. 52, pp. 1851–1862, Nov. 2005.
[5] Y. Liang, J. Caverlee, and C. Cao, ''A noise-filtering approach for spatio-temporal event detection in social media,'' in *Proc. Eur. Conf. Inf. Retr.*, Mar. 2015, pp. 233–244.
[6] L. A. Jeni and A. Lorincz, Z. Szabó, J. F. Cohn, and T. Kanade, ''Spatio-temporal event classification using time-series kernel based structured sparsity,'' in *Proc. Eur. Conf. Comput. Vis.*, Sep. 2016, pp. 135–150.
[7] S. Sathya and D. Sundararajan, ''Improved wavelet based detection of power quality events in the presence of noise,'' in *Proc. Int. Conf. Circuits, Power Comput. Technol.*, Mar. 2015, pp. 1–6.
[8] H. Zhou, S. Xu, D. Ren, C. Huang, and H. Zhang, ''Analysis of event-driven warning message propagation in vehicular ad hoc networks,'' *Ad Hoc Netw.*, vol. 55, pp. 87–96, Feb. 2017.
[9] D. Xu, Y. Qin, H. Zhang, L. Yu, and H. Wang, ''Set-valued kalman filtering: Event triggered communication with quantized measurements,'' in *Peer-to-Peer Networking and Applications*. Springer, 2018, pp. 1–12.
[10] S. Grziwa and M. Pätzold, (2016). ''Wavelet-based filter methods to detect small transiting planets in stellar light curves.'' [Online]. Available: https://arxiv.org/abs/1607.08417
[11] X. Ge, Q.-L. Han, and B. Liu, ''Distributed H_∞ filtering of discrete-time linear systems over sensor networks with event-triggered communication,'' in *Proc. IEEE 13th Int. Conf. Ind. Inform.*, Oct. 2015, pp. 156–161.
[12] X. Ge and Q. L. Han, ''Distributed event-triggered H_∞ filtering over sensor networks with communication delays,'' *Inf. Sci.*, vol. 291, pp. 128–142, Sep. 2015.
[13] Y. Zhu, Z. Zhong, H. Zhang, and D. Zhou, ''Filtering for networked switched systems with multiple redundant channels: An application to the boost-buck converter,'' in *Proc. 13th IEEE Int. Conf. Control Automat. (ICCA)*, Jul. 2017, pp. 594–599.
[14] H. Zhang *et al.*, ''Optimal DoS attack scheduling in wireless networked control system,'' *IEEE Trans. Control Syst. Technol.*, vol. 24, no. 3, pp. 843–852, May 2016.
[15] S. Trimpe, ''Event-based state estimation: An emulation-based approach,'' *IET Control Theory Appl.*, vol. 11, no. 11, pp. 1684–1693, Jul. 2017.

[16] S. Wang, Y. Wang, Y. Jiang, and Y. Li, "Event-triggered based distributed h_∞ consensus filtering for discrete-time delayed systems over lossy sensor network," *Trans. Inst. Meas. Control*, vol. 40, no. 9, pp. 2740–2747, Jun. 2018.
[17] M. Rashedi, J. Liu, and B. Huang, "Triggered communication in distributed adaptive high-gain EKF," *IEEE Trans. Ind. Informat.*, vol. 14, no. 1, pp. 58–68, Jan. 2018.
[18] L. Wang, Z. Wang, Q.-L. Han, and G. Wei, "Event-based variance-constrained H_∞ filtering for stochastic parameter systems over sensor networks with successive missing measurements," *IEEE Trans. Cybern.*, vol. 48, no. 3, pp. 1007–1017, Mar. 2018.
[19] M. Ghodrat and H. J. Marquez, "On the local input–output stability of event-triggered control systems," *IEEE Trans. Autom. Control*, vol. 64, no. 1, pp. 174–189, Jan. 2019. [Online]. Available: https://ieeexplore.ieee.org/document/8302522
[20] S. H. Mousavi and H. J. Marquez, "Integral-based event triggering controller design for stochastic LTI systems via convex optimisation," *Int. J. Control*, vol. 89, no. 7, pp. 1416–1427, 2016.
[21] K. J. Åström, and B. Bernhardsson, "Comparison of periodic and event based sampling for first-order stochastic systems," in *Proc. 14th World Congr. IFAC*, Jul. 1999, pp. 301–306.
[22] P. Tabuada, "Event-triggered real-time scheduling of stabilizing control tasks," *IEEE Trans. Autom. Control*, vol. 52, no. 9, pp. 1680–1685, Sep. 2007.
[23] X. Wang and M. D. Lemmon, "Event-triggering in distributed networked control systems," *IEEE Trans. Autom. Control*, vol. 56, no. 3, pp. 586–601, Mar. 2011.
[24] R. Postoyan, P. Tabuada, and D. Nešic, and A. Anta, "A framework for the event-triggered stabilization of nonlinear systems," *IEEE Trans. Autom. Control*, vol. 60, no. 4, pp. 982–996, Apr. 2015.
[25] D. Shi, T. Chen, and L. Shi, "Event-triggered maximum likelihood state estimation," *Automatica*, vol. 50, no. 1, pp. 247–254, Jan. 2014.
[26] S. Trimpe and R. D'Andrea, "Event-based state estimation with variance-based triggering," *IEEE Trans. Autom. Control*, vol. 59, no. 12, pp. 3266–3281, Dec. 2014.
[27] D. Han, Y. Mo, J. Wu, S. Weerakkody, B. Sinopoli, and L. Shi, "Stochastic event-triggered sensor schedule for remote state estimation," *IEEE Trans. Autom. Control*, vol. 60, no. 10, pp. 2661–2675, Oct. 2015.
[28] S. Hu, Y. Zhang, and Z. Du, "Network-based H_∞ tracking control with event-triggering sampling scheme," *IET Control Theory Appl.*, vol. 6, no. 4, pp. 533–544, 2012.
[29] S. Hu and D. Yue, "Event-based H_∞ filtering for networked system with communication delay," *Signal Process.*, vol. 92, no. 9, pp. 2029–2039, 2012.
[30] X.-M. Zhang and Q.-L. Han, "Event-based H_∞ filtering for sampled-data systems," *Automatica*, vol. 51, no. 1, pp. 55–69, Jan. 2015.
[31] J. Wang, X.-M. Zhang, and Q.-L. Han, "Event-triggered generalized dissipativity filtering for neural networks with time-varying delays," *IEEE Trans. Neural Netw. Learn. Syst.*, vol. 27, no. 1, pp. 77–88, Jan. 2016.
[32] J. Shiles *et al.*, "Microgrid protection: An overview of protection strategies in North American microgrid projects," in *Proc. IEEE Power Energy Soc. Gen. Meeting*, Feb. 2018, pp. 1–5.
[33] M. Davari and Y. A.-R. I. Mohamed, "Robust multi-objective control of VSC-based DC-voltage power port in hybrid AC/DC multi-terminal microgrids," *IEEE Trans. Smart Grid*, vol. 4, no. 3, pp. 1597–1612, Sep. 2013.
[34] F. Katiraei, R. Iravani, N. Hatziargyriou, and A. Dimeas, "Microgrids management: Controls and operation aspects of microgrids," *IEEE Power Energy Mag.*, vol. 6, no. 3, pp. 54–65, Sep. 2008.
[35] T. Ersal *et al.*, "Coupling between component sizing and regulation capability in microgrids," *IEEE Trans. Smart Grid*, vol. 4, no. 3, pp. 1576–1585, Sep. 2013.
[36] Advancing Energy Storage Technology in California. *California Energy Storage Showcase*. [Online]. Available: http://www.energy.ca.gov/research/energystorage/tour/
[37] U.K. Government's National Statistics. *Renewables Statistics Collection*. Accessed: Sep. 26, 2013. [Online]. Available: https://www.gov.uk/government/collections/renewables-statistics
[38] U.S. Department of Energy. *The War of the Currents: AC vs. DC Power*. Accessed: Nov. 18, 2014. [Online]. Available: http://energy.gov/articles/war-currents-ac-vs-dc-power
[39] Federal Energy Regulatory Commission. *Energy Independence and Security Act of 2007 Title XIII Smart Grid*. Accessed: 2007. [Online]. Available: https://www.ferc.gov/industries/electric/indus-act/smart-grid/eisa.pdf
[40] G. R. Grimmett and D. R. Stirzaker, *Probability and Random Processes*. Oxford, U.K.: Clarendon, 1992.
[41] S. Hu and D. Yue, "Event-based H_∞ filtering for networked systems with communication delay," *Signal Process.*, vol. 92, no. 9, pp. 2029–2039, 2012.
[42] K. E. Atkinson, *An Introduction to Numerical Analysis*. Hoboken, NJ, USA: Wiley, 1989.
[43] M. Wu, Y. He, J.-H. She, and G.-P. Liu, "Delay-dependent criteria for robust stability of time-varying delay systems," *Automatica*, vol. 40, no. 8, pp. 1435–1439, 2004.
[44] S. Boyd and L. Vandenberghe, *Convex Optimization*. Cambrige, U.K.: Cambrige Univ. Press, 2004.
[45] M. Davari and F. Katiraei, "Investigation and correction of phase shift delays in power hardware in loop real-time digital simulation testing of power electronic converters," in *Proc. Grid Future Symp. (CIGRE US Nat. Committee)*, Oct. 2015, pp. 1–11.
[46] M. Davari, "Dynamics of an industrial power amplifier for evaluating PHIL testing accuracy: An experimental approach via linear system identification methods," in *Proc. IEEE Int. Conf. Ind. Electron. Sustain. Energy Syst.*, Feb. 2018, pp. 540–545.
[47] HIL402. *Typhoon Inc*. [Online]. Available: https://www.typhoon-hil.com/products/hil402
[48] P. C. Krause, O. Wasynczuk, S. D. Sudhoff, and S. Pekarek, *Analysis of Electric Machinery and Drive Systems*. Hoboken, NJ, USA: Wiley, 2013.
[49] S. J. Sørås, "Frequency regulation of synchronous generator," M.S. thesis, Geophys. Inst. Univ. Bergen, Bergen, Norway, Jun. 2017.
[50] E. Johansson, "Detailed description of synchronous machine models used in simpow," M.S. thesis, Dept. Elect. Eng., KTH Roy. Inst. Technol., Stockholm, Sweden, 2002.

SEYED HOSSEIN MOUSAVI (M'17) was born in Shiraz, Iran. He received the B.Sc. and M.Sc. degrees in electrical engineering-control from Shiraz University, Shiraz, Iran, in 2008 and 2011, respectively, and the Ph.D. degree in electrical engineering-control systems from the University of Alberta, Edmonton, AB, Canada, in 2016.

He was as a Postdoctoral Researcher with the Department of Aerospace Engineering, Ryerson University, Toronto, Canada, from 2016 to 2018. He is currently with Niigon Machines, Ltd., Vaughan, ON, Canada.

MASOUD DAVARI (S'08–M'17) was born in Isfahan, Iran, in 1985. He received the B.Sc. degree (Hons.) in electrical engineering-power from the Isfahan University of Technology, Isfahan, Iran, in 2007, the M.Sc. degree (Hons.) in electrical engineering-power from the Amirkabir University of Technology (Tehran Polytechnic), Tehran, Iran, in 2010, and the Ph.D. degree in electrical engineering-energy systems from the University of Alberta, Edmonton, AB, Canada, in 2016.

He has been with Iran's Grid Secure Operation Research Center and Iran's Electric Power Research Institute, Tehran, Iran, from 2010 to 2011. From 2015 to 2017, he was collaborating with Quanta-Technology Company in dynamic interaction of renewable energy systems with smart grids and control, protection, and automation of microgrids as a Senior R & D Specialist and a Senior Consultant. Since 2017, he has been with the Department of Electrical and Computer Engineering, Allen E. Paulson College of Engineering and Computing, Georgia Southern University, Statesboro, GA, USA as a tenure-track Assistant Professor Faculty Member. His research interests include the dynamics, controls, and protections of different types of power electronic converters, which are employed in the hybrid ac/dc smart grids, and hardware-in-the-loop (HIL) testing of modernized power systems.

Dr. Davari is an Invited Member of the Golden Key International Honour Society. He has been an Active Member and a Chapter Lead (for Chapter 3) in the IEEE WG P2004, a newly established IEEE working group on the HIL simulation for IEEE Standards Association, since 2017. He served as the Chair of the Literature Review Subgroup of DC@home Standards for IEEE Standards Association, from 2014 to 2015. He has developed and implemented several experimental test rigs for both research universities and the industry. He has authored, an Invited Reviewer, and the Invited Speaker of several IEEE Transactions and journals, IET journals, *Energies* journal, various conferences, and diverse universities and places from different societies.

HORACIO J. MARQUEZ (SM'08) received the B.Sc. degree from the Instituto Tecnológico de Buenos Aires, Argentina, in 1987, and the M.Sc.E. and Ph.D. degrees in electrical engineering from the University of New Brunswick, Fredericton, Canada, in 1990 and 1993, respectively.

From 1993 to 1996, he held visiting appointments at the Royal Roads Military College, and the University of Victoria, Victoria, BC, Canada. Since 1996, he has been with the Department of Electrical and Computer Engineering, University of Alberta, Edmonton, Canada, where he is currently a Professor. From 2000 to 2004, he was an Associate Chair of Graduate Studies, and from 2004 to 2014, he was a Chair of electrical and computer engineering. In 2008, he was a Guest Research Professor with Nancy University University Henri Poincaré, France. His current research interests include nonlinear dynamical systems and control, nonlinear observer design, sampled-data systems, and control of cyber-physical systems.

Dr. Marquez was a recipient of the 2003–2004 McCalla Research Professorship received by the University of Alberta. He is currently an Area Editor for the *International Journal of Robust and Nonlinear Control* and an Associate Editor of the IEEE Control Systems Letters and *IET-Control Theory & Applications*. He has authored the book *Nonlinear Control Systems: Analysis and Design* (Wiley, 2003). He is a Licensed Professional Engineer (P.Eng.) in the Province of Alberta and is a Fellow of IET (formerly IEE), the Canadian Academy of Engineering, and the Engineering Institute of Canada.